Universität Potsdam

Fred Feudel, Norbert Seehafer, Olaf Schmidtmann

Fluid helicity and dynamo bifurcations

NLD Preprints ; 18

Fluid helicity and dynamo bifurcations

Fred Feudel, Norbert Seehafer, Olaf Schmidtmann

Max-Planck-Gruppe Nichtlineare Dynamik, Universität Potsdam, PF 601553, D-14415 Potsdam, Germany

Abstract

The bifurcation behaviour of the 3D magnetohydrodynamic equations has been studied for external forcings of varying degree of helicity. With increasing strength of the forcing a primary non-magnetic steady state loses stability to a magnetic periodic state if the helicity exceeds a threshold value and to different non-magnetic states otherwise.

1. Introduction

A prominent objective in the theory of electrically conducting fluids is the explanation of the origin of the cosmical magnetic fields, such as those of the Earth and the Sun (for a recent account of the subject see e.g. Ref. [1]). The majority of studies in this field has been kinematic. Kinematic dynamo theory studies the conditions under which a prescribed velocity field can amplify, or at least prevent from decaying, some seed magnetic field, completely disregarding the equations governing the motion of the fluid. The hitherto most successful branch of kinematic dynamo theory is the theory of the turbulent dynamo [2, 3], which has supplied evidence that the presence of kinetic and magnetic helicities is favourable for a dynamo effect. With $\mathbf{v}$, $\mathbf{B}$ and $\mathbf{A}$ denoting fluid velocity, magnetic field and a magnetic vector potential, the densities per unit volume of kinetic and magnetic helicity are defined by

$$H_K = \mathbf{v} \cdot \operatorname{curl} \mathbf{v}, \quad H_M = \mathbf{A} \cdot \mathbf{B}. \tag{1}$$

Simple examples of strongly helical flows are provided by the so-called ABC flows,

$$\mathbf{v} = \mathbf{v}_{ABC} = (A \sin z + C \cos y,\ B \sin x + A \cos z,\ C \sin y + B \cos x), \tag{2}$$

where A, B and C denote constant coefficients. By satisfying $\operatorname{curl} \mathbf{v} = \mathbf{v}$, they have the Beltrami property, $\operatorname{curl} \mathbf{v} \times \mathbf{v} = \mathbf{0}$, and in general (if $ABC \neq 0$), there are domains in the flow where the streamlines are chaotic. For these reasons, they have received much interest [4, 5, 6], notably as candidates for fast dynamos (kinematic dynamos for which the growth rate of the magnetic field remains bounded away from zero as the magnetic diffusivity tends to zero). The ABC flows are steady solutions of the incompressible Euler equations. They are also steady solutions of the incompressible Navier–Stokes equations if an external body force

$$\mathbf{f} = -\nu \Delta \mathbf{v}_{ABC} = \nu \mathbf{v}_{ABC} \tag{3}$$

just compensating for viscous losses (see Eq. (4) below) is applied; in this case they are stable below und unstable above a certain critical strength of the forcing or

critical Reynolds number, respectively [7, 8]. Imposing this kind of forcing, Galanti et al. [9] studied the complete system of the incompressible magnetohydrodynamic (MHD) equations. Numerically simulating the system for selected Reynolds numbers and selected initial conditions, they observed that at some critical value of the Reynolds number a stable ABC flow without a magnetic field loses stability to a time-periodic state with a magnetic field. In the present paper we continue the study of Galanti et al. by systematically applying numerical methods of bifurcation analysis. In particular, by varying the degree of helicity in the forcing, we check the role of helicity for a dynamo effect.

2. Basic equations, truncation, and forcing

We start from the incompressible non-relativistic MHD equations,

$$\frac{\partial \mathbf{v}}{\partial t} + (\mathbf{v}\cdot\nabla)\mathbf{v} = \nu\Delta\mathbf{v} - \operatorname{grad} p - \frac{1}{2}\operatorname{grad}\mathbf{B}^2 + (\mathbf{B}\cdot\nabla)\mathbf{B} + \mathbf{f}, \tag{4}$$

$$\frac{\partial \mathbf{B}}{\partial t} + (\mathbf{v}\cdot\nabla)\mathbf{B} = \eta\Delta\mathbf{B} + (\mathbf{B}\cdot\nabla)\mathbf{v}, \tag{5}$$

$$\operatorname{div}\mathbf{v} = 0, \quad \operatorname{div}\mathbf{B} = 0, \tag{6}$$

where the density has been set equal to unity, ν and η denote the (constant) kinematic viscosity and magnetic diffusivity, respectively, p is the thermal pressure, and $\mathbf{f}$ an external body force (see e.g. Ref. [10]).

We apply periodic boundary conditions on a cube of side length 2π, which is equivalent to considering the motion on the torus $T^3 = [0,2\pi]\times[0,2\pi]\times[0,2\pi]$. The mean values of $\mathbf{v}$ and $\mathbf{B}$, and consequently also of $\mathbf{f}$, are assumed to vanish,

$$\int_{T^3}\mathbf{v}\,\mathrm{d}^3\mathbf{x} = \mathbf{0}, \quad \int_{T^3}\mathbf{B}\,\mathrm{d}^3\mathbf{x} = \mathbf{0}, \quad \int_{T^3}\mathbf{f}\,\mathrm{d}^3\mathbf{x} = \mathbf{0}. \tag{7}$$

Let $\mathbf{v}_\mathbf{k}$, $\mathbf{B}_\mathbf{k}$, $p_\mathbf{k}$ and $\mathbf{f}_\mathbf{k}$ denote the Fourier coefficients of $\mathbf{v}$, $\mathbf{B}$, p and $\mathbf{f}$ for wave number $\mathbf{k}\in\mathbb{Z}^3$, $\mathbf{k}\neq 0$. In Fourier space Eq. (6) takes the form

$$\mathbf{v}_\mathbf{k}\cdot\mathbf{k} = 0, \quad \mathbf{B}_\mathbf{k}\cdot\mathbf{k} = 0 \tag{8}$$

and is automatically satisfied if we write

$$\mathbf{v}_\mathbf{k} = v_\mathbf{k}^{(1)}\mathbf{e}_\mathbf{k}^{(1)} + v_\mathbf{k}^{(2)}\mathbf{e}_\mathbf{k}^{(2)}, \quad \mathbf{B}_\mathbf{k} = B_\mathbf{k}^{(1)}\mathbf{e}_\mathbf{k}^{(1)} + B_\mathbf{k}^{(2)}\mathbf{e}_\mathbf{k}^{(2)} \qquad \text{for } \mathbf{k}\neq\mathbf{0}, \tag{9}$$

with (real) "polarization" unit vectors $\mathbf{e}_\mathbf{k}^{(1)}$, $\mathbf{e}_\mathbf{k}^{(2)}$ perpendicular to $\mathbf{k}$,

$$\mathbf{e}_\mathbf{k}^{(i)}\cdot\mathbf{k} = 0, \quad \mathbf{e}_\mathbf{k}^{(1)}\cdot\mathbf{e}_\mathbf{k}^{(2)} = 0, \quad \mathbf{e}_\mathbf{k}^{(i)}\cdot\mathbf{e}_\mathbf{k}^{(i)} = 1, \quad \mathbf{e}_{-\mathbf{k}}^{(i)} = \mathbf{e}_\mathbf{k}^{(i)}, \qquad i = 1,2. \tag{10}$$

By using these representations for $\mathbf{v}_\mathbf{k}$ and $\mathbf{B}_\mathbf{k}$ we furthermore get rid of both the thermal, $\operatorname{grad} p$, and magnetic, $\operatorname{grad}\mathbf{B}^2/2$, pressure terms in Eq. (4) and arrive at the following infinite-dimensional system of ODE:

$$\frac{\mathrm{d}v_\mathbf{k}^{(j)}}{\mathrm{d}t} = -\nu\mathbf{k}^2 v_\mathbf{k}^{(j)} - \mathrm{i}\sum_{\substack{\mathbf{p}\in\mathbb{Z}^3\\ \mathbf{p}\neq\mathbf{0},\mathbf{k}}}\sum_{\alpha,\beta=1}^{2}(\mathbf{e}_\mathbf{p}^{(\alpha)}\cdot\mathbf{e}_\mathbf{k}^{(j)})(\mathbf{e}_{\mathbf{k}-\mathbf{p}}^{(\beta)}\cdot\mathbf{k})[v_\mathbf{p}^{(\alpha)}v_{\mathbf{k}-\mathbf{p}}^{(\beta)} - B_\mathbf{p}^{(\alpha)}B_{\mathbf{k}-\mathbf{p}}^{(\beta)}] + f_\mathbf{k}^{(j)}, \tag{11}$$

$$\frac{\mathrm{d}B_{\mathbf{k}}^{(j)}}{\mathrm{d}t} = -\eta \mathbf{k}^2 B_{\mathbf{k}}^{(j)} - \mathrm{i} \sum_{\substack{\mathbf{p}\in\mathbb{Z}^3 \\ \mathbf{p}\neq\mathbf{0},\mathbf{k}}} \sum_{\alpha,\beta=1}^{2} (\mathbf{e}_{\mathbf{p}}^{(\alpha)} \cdot \mathbf{e}_{\mathbf{k}}^{(j)})(\mathbf{e}_{\mathbf{k}-\mathbf{p}}^{(\beta)} \cdot \mathbf{k})[B_{\mathbf{p}}^{(\alpha)} v_{\mathbf{k}-\mathbf{p}}^{(\beta)} - v_{\mathbf{p}}^{(\alpha)} B_{\mathbf{k}-\mathbf{p}}^{(\beta)}]. \quad (12)$$

$f_{\mathbf{k}}^{(j)}$ on the right of Eq. (11) is defined by

$$f_{\mathbf{k}}^{(j)} = \mathbf{f}_{\mathbf{k}} \cdot \mathbf{e}_{\mathbf{k}}^{(j)}, \qquad j = 1, 2. \quad (13)$$

In our numerical calculations, an isotropic truncation in wave number space has been used, following Lee [11, 12], who segmented $\mathbf{k}$ space into successive shells $n^2 - n < \mathbf{k}^2 \leq n^2 + n$, $n = 1, 2, \cdots$. In most of our calculations we have taken into account three shells, corresponding to 89 $\mathbf{k}$-vectors, which amounts to studying a system of 712 ODE. But partially, to test the influence of the degree of truncation, up to 9 shells were included in the computations, corresponding to 1847 $\mathbf{k}$-vectors and 14776 ODE, respectively.

Our forcing has been a generalisation of the ABC forcing (Eq. (3)), given by

$$\mathbf{f} = \nu((1-\lambda)\mathbf{v}_{ABC} + \lambda \mathbf{v}_{ABC}^{-}), \quad (14)$$

where

$$\mathbf{v}_{ABC}^{-} = (-A\cos z - C\sin y,\ -B\cos x - A\sin z,\ -C\cos y - B\sin x) \quad (15)$$

and λ is a parameter varying between 0 and 0.5. $\mathbf{v}_{ABC}^{-}$ satisfies $\operatorname{curl} \mathbf{v}_{ABC}^{-} = -\mathbf{v}_{ABC}^{-}$, and for $\lambda = 0.5$ its addition in the forcing term "kills" the helicity on average in the volume, while $\lambda = 0$ corresponds to the original ABC forcing.

Restricting ourselves to the case

$$A = B = C = f, \quad \nu = \eta, \quad (16)$$

we have, following Galanti et al. [9], defined a Reynolds number

$$R = \frac{f}{\nu} = \frac{f}{\eta}. \quad (17)$$

R and λ have been our bifurcation parameters.

3. Results

For weak forcing (small R), there exists a stable stationary solution — in the case of $\lambda = 0$ just the ABC flow — with vanishing magnetic field, and all system trajectories are attracted by this solution. While keeping fixed the value of λ, we have traced the steady-solution branch for varying R by means of a predictor-corrector method, in each step calculating, in order to detect bifurcation points, the eigenvalues of the Jacobian matrix. For $\lambda < 0.4$ the steady state loses stability in a Hopf bifurcation. Table 1 summarizes for the case of $\lambda = 0$ the values of the Reynolds number at which the Hopf bifurcation appears for different truncations. A dependence of the

Number of shells in **k** space	Number of modes (equations)		Critical R for Hopf bifurcation
2	40	(320)	4.6
3	89	(712)	5.7
4	194	(1552)	12.7
5	369	(2952)	8.2
6	594	(4752)	<12.5
7	895	(7160)	<11.0
9	1847	(14776)	<12.0

Table 1: Reynolds number at which the Hopf bifurcation was observed for different truncations in wave number space in the case of $\lambda = 0$.

critical Reynolds number on the degree of truncation is discernible, with a tendency to higher values for weaker truncation. The latter may be due to an increase of the energy dissipation with increasing number of modes. Because of a very long run time of the program calculating the eigenvalues of the Jacobian matrix, for the cases with more than 5 shells in **k** space only upper bounds for the critical Reynolds number are given, obtained from simulations of single trajectories.

In the following we present results obtained by applying the three-shell truncation. These are likely to be representative of the system at least for Reynolds numbers not too far above the critical value for the first bifurcation of the original steady state.

The type of the first bifurcation, as well as the character of the time-asymptotic states after this bifurcation, change at $\lambda = 0.4$. While for $\lambda < 0.4$ a magnetic periodic state is the (only) new attractor, for λ between 0.4 and 0.5 new non-magnetic states emerge.

The original steady state has been traced also in the region beyond the first bifurcation, where it is unstable and where it undergoes secondary bifurcations. The locations of primary and secondary bifurcations in the parameter plane are shown in Fig. 1. Thick solid and dashed lines, respectively, indicate the primary bifurcation of the original steady state. For $0.4 < \lambda < 0.49$ the Hopf bifurcation is preceded by a bifurcation in which two real eigenvalues of the Jacobian matrix become positive; these two eigenvalues are equal already before the bifurcation, due to one of the symmetries in the system. The bifurcation results in three coexisting new stable stationary solutions, which can be transformed into each other by certain elements of the symmetry group of our problem (which is a subgroup of the symmetry group of the MHD equations with the original ABC forcing [5]). For $\lambda = 0.4$ this bifurcation occurs simultaneously with the Hopf bifurcation.

At $\lambda = 0.49$, showing up as a kind of cusp in Fig. 1, the primary bifurcation changes its character again, namely from the real bifurcation observed for $\lambda < 0.49$ to another Hopf bifurcation for $\lambda > 0.49$. This Hopf bifurcation leads to a non-magnetic periodic state. At the cusp-like transition point the imaginary part of the

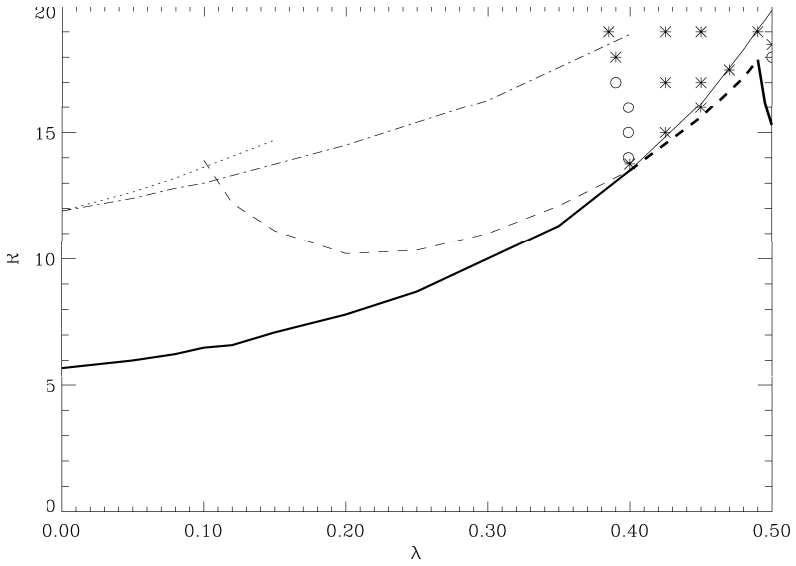

Figure 1: Locations of primary and secondary bifurcations of the original stationary solution in the λ-R plane. Solid line and dashed-dotted line: a single pair of complex conjugate eigenvalues crosses the imaginary axis; dashed line: two real eigenvalues pass through zero; dotted line: two pairs of complex conjugate eigenvalues cross the imaginary axis. Asterisks indicate points at which, by means of simulations, non-magnetic chaotic (Shilnikov-like) time-asymptotic states have been found, while circles correspond to magnetic periodic attractors.

pair of complex-conjugate eigenvalues responsible for the Hopf bifurcation to the right is zero, and the complex-conjugate pair coincides with the real pair responsible for the bifurcation to the left.

The new stationary and periodic solutions bifurcating from the original stationary one for $0.4 < \lambda < 0.5$ are stable only over very small intervals of the bifurcation parameter R and lose their stability directly to non-magnetic chaotic states. The presence of chaos has been verified by calculating, for selected values of the bifurcation parameters, the largest Lyapunov exponents. For these calculations we have used the algorithm of Shimada and Nagashima [13]. Fig. 2 shows for $\lambda = 0.45$ and

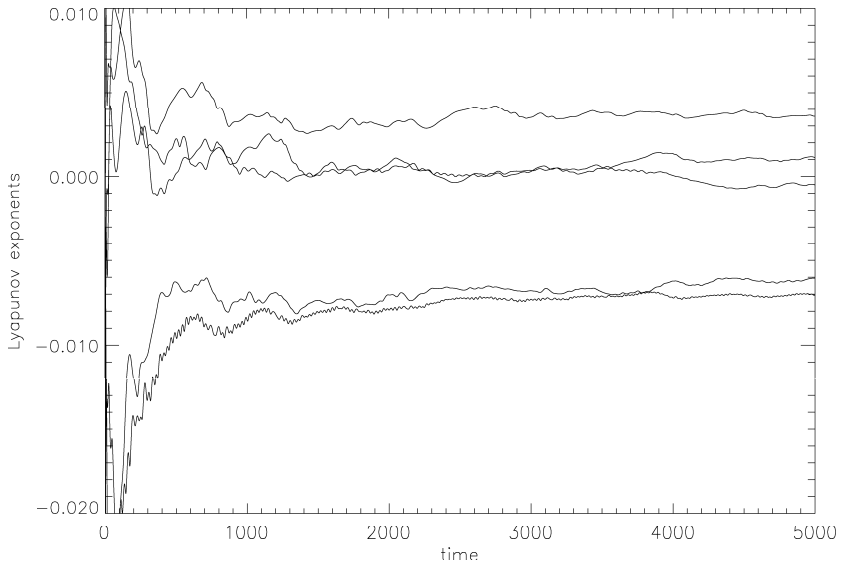

Figure 2: The 5 largest Lyapunov exponents for $\lambda = 0.45$ and $R = 17$.

$R = 17$ the 5 largest Lyapunov exponents in dependence on the integration time. A good convergence is discernible, as well as that at least one exponent is positive.

The chaotic attractors found here look all similar. They are strongly suggestive of Shilnikov-type homoclinic chaos (see Fig. 3) and their appearance seems to be connected with the degenerate bifurcation at $\lambda = 0.4$ (crossing of solid and dashed line in Fig. 1). In problems with two parameters, the occurence of homoclinic orbits in the vicinity of such points of degeneracy is a generic phenomenon (see e.g. Ref. [14]).

In Fig. 1, asterisks indicate points at which non-magnetic Shilnikov-like chaotic attractors have been found. The non-magnetic chaotic domain extends also to λ values less than 0.4, there causing a disappearance of the dynamo effect already present at smaller Reynolds numbers, which is reminiscent of the "windows" in dynamo action found in kinematic studies [6].

Finally, we wish to emphasize that in the present paper we have dealt with the behaviour of our system only for Reynolds numbers below or slightly above the first

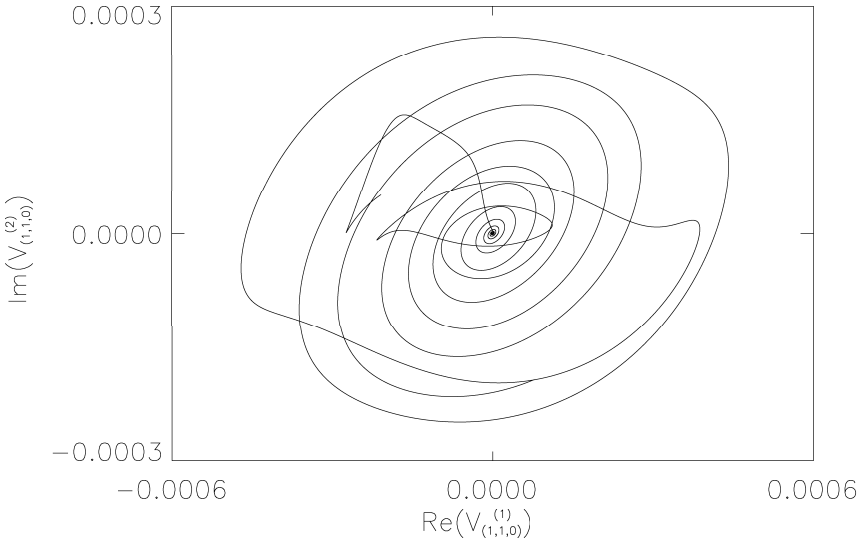

Figure 3: Chaotic attractor for $\lambda = 0.45$ and $R = 17$.

bifurcation value. Subsequent bifurcations, as well as the role of the symmetries in the system, are presently under investigation.

4. Conclusion

It has been shown by a bifurcation study of the complete system of the MHD equations with a generalised ABC forcing that the transition from an always existing stable stationary solution to time-dependent states is decisively influenced by the degree of helicity in the forcing. If the helicity exceeds a certain threshold value, a Hopf bifurcation leads to a magnetic periodic state (dynamo effect). For helicities below the threshold value the transition is more complex, but always the ensuing time-dependent states (including chaotic ones) are non-magnetic.

Acknowledgement

We would like to thank M. Zaks for many helpful discussions.

References

[1] P.H. Roberts and A.M. Soward, Ann. Rev. Fluid Mech. 24 (1992) 459.

[2] H.K. Moffatt, Magnetic field generation in electrically conducting fluids (Cambridge Univ. Press, Cambridge, 1978).

[3] F. Krause and K.-H. Rädler, Mean-field magnetohydrodynamics and dynamo theory (Akademie-Verlag, Berlin, 1980).

[4] V.I. Arnold and E.I. Korkina, Vest. Mosk. Univ. Mat. Mekh. 3 (1983) 43.

[5] T. Dombre, U. Frisch, J.M. Greene, M. Hénon, A. Mehr and A.M. Soward, J. Fluid Mech. 167 (1986) 353.

[6] D. Galloway and U. Frisch, Geophys. Astrophys. Fluid Dyn. 36 (1986) 53.

[7] D. Galloway and U. Frisch, J. Fluid Mech. 180 (1987) 557.

[8] O. Podvigina and A. Pouquet, Physica D 75 (1994) 471.

[9] B. Galanti, P.L. Sulem and A. Pouquet, Geophys. Astrophys. Fluid Dyn. 66 (1992) 183.

[10] P.H. Roberts, An introduction to magnetohydrodynamics (Longmans, London, 1967).

[11] J. Lee, Physica D 37 (1989) 417.

[12] J. Lee, Chaos 2 (1992) 537.

[13] I. Shimada and T. Nagashima, Progr. Theor. Phys. 61 (1979) 1605.

[14] G. Nicolis and P. Gaspard, in: Continuations and bifurcations: Numerical techniques and applications, eds. D. Roose, B. de Dier and A. Spence (Kluwer, Dordrecht, 1990) p. 43.